Progress In Electromagnetics Research M, Vol. 68, 69–77, 2018

A Compact Dual Band MIMO Antenna with Improved Isolation for WI-MAX and WLAN Applications

Pratima C. Nirmal[1, *], Anil Nandgaonkar[1], Sanjay Nalbalwar[1], and Rajiv K. Gupta[2]

Abstract—In this paper, a compact dual-band MIMO antenna for WI-MAX and WLAN applications with improved isolation is proposed. The proposed design consists of two counter facing F shaped monopoles placed closely to each other with edge to edge spacing of 10 mm ($0.1167\lambda_0$ at 3.5 GHz). Each monopole element operates over 3.5 and 5.8 GHz bands. The isolation over the operating dual bands is achieved by using an elliptical slot and a rectangular parasitic strip. $S_{11} < -10\,\text{dB}$ is achieved over 3.2–3.8 GHz and 5.7–6.2 GHz with $S_{12} < -20\,\text{dB}$. The overall dimension of the proposed antenna is $30 \times 26\,\text{mm}^2$. The proposed antenna has correlation coefficient < 0.03, diversity gain $> 9.8\,\text{dB}$ with stable radiation pattern over the operating dual bands. The measured results are in good agreement with the simulated ones. The proposed antenna is a suitable candidate for MIMO applications.

1. INTRODUCTION

With recent growth in today's requirement for increased data rate, huge capacity and high throughput, a single antenna system was deprived of fulfilling the desired requirement as it was more prone to multipath fading and had low data rate [1]. These drawbacks have been overcome by MIMO antenna system. MIMO system uses more than one antenna elements for communicating the signals. MIMO antenna has been gaining importance in wireless communication system due to its benefits such as low multipath fading, increased capacity, higher data rates, lower signal loss, and low co-channel interference. The main challenge in the design of MIMO antenna is to achieve high isolation among the multiple antenna elements and to develop a compact size MIMO antenna [2]. When many antenna elements are placed together, the antenna radiation characteristics get degraded due to high mutual coupling effects. So perseverance of radiation characteristics are also required. Moreover, to design a dual-band antenna for MIMO applications is a difficult task. The design complexity lies in achieving high isolation between two different resonant bands of compact MIMO antennas.

An electrically small and compact antenna using artificial materials is designed and discussed in [3] while a dual-broadband antenna using compact double split ring resonators is reported in [4]. Various dual-band MIMO antennas have been reported in [5–14]. A neutralization line is placed in between two dual-band monopole antennas to improve the isolation greater than 15 dB [5]. This line act as an inductance to nullify the capacitance between the antenna elements. In [6], a T-shape stub and rectangular slots are used for achieving the mutual coupling $< -20\,\text{dB}$. The distance between the antennas and slot dimensions is also optimized for achieving high isolation over dual operating bands. The dual-band MIMO system in [7] has a stub at the center of ground plane and a slot which results in isolation of more than 15 dB. A different technique consisting of a modified T-shape resonator with a rectangular loop is used to attain the isolation above 15 dB in [8]. High isolation in dual-band MIMO antennas is achieved by orthogonally arranging the antenna elements [9]. These orthogonal placed

---

Received 31 March 2018, Accepted 25 April 2018, Scheduled 7 May 2018

[*] Corresponding author: Pratima Chabbilal Nirmal (pratima.nirmal@gmail.com).

[1] Department of Electronics and Telecommunication, DBATU, Lonere, Raigad, India. [2] Department of Electronics and Telecommunication, Terna Engineering College, Navi-Mumbai, India.

antenna elements are fed by a coplanar waveguide line. A dual-band array fabricated on an FR-4 substrate with a stub and strip for WLAN application is reported in [10]. In [11], slotted CSRR whose operating frequency is varied by changing the slot length is used to improve the isolation. In [12], isolation $> 20\,\text{dB}$ is achieved between the MIMO antennas by placing a transmission line above the substrate and using slots in the ground. Slot antennas with decoupling structures are proposed to have $S_{12} < -20\,\text{dB}$ for 2.4/5.8 GHz WLAN applications [13]. Further in [14], a CPW-fed trapezoid-shaped MIMO antenna with ring-shaped ground plane is designed for WI-MAX and WLAN applications with mutual coupling less than $-20\,\text{dB}$. All the above mentioned structures have large dimensions compared to our proposed structure.

In this paper, a dual-band MIMO antenna with improved isolation is proposed. The proposed structure consists of two counter facing F-shaped monopoles placed closely to each other with edge to edge spacing of $0.1167\lambda_0$ at 3.5 GHz. The isolation over dual bands is achieved by using an elliptical slot and a rectangular parasitic strip. $S_{11} < -10\,\text{dB}$ is obtained over 3.2–3.8 GHz and 5.7–6.2 GHz with $S_{12} < -20\,\text{dB}$. The dimension of the proposed antenna design is $30 \times 26\,\text{mm}^2$, and the antenna is fabricated using a 1.6 mm thick FR-4 substrate. Moreover, correlation coefficient is less than 0.03 with stable radiation pattern over the operating bands. The proposed antenna is suitable for WI-MAX and WLAN applications. Following section deals with antenna design, simulation results and conclusion.

2. ANTENNA GEOMETRY AND DESIGN THEORY

Initially, Ant A consisting of a rectangular monopole of length 'L' and width 'W' is designed. The lower resonating frequency of rectangular monopole antenna (f_L) is calculated using Equation (1) [15]:

$$f_L = \frac{c}{\lambda} = \frac{7.2}{\left(L + g + \dfrac{W}{2\pi}\right)} \tag{1}$$

where g is the gap between the monopole and the ground plane. The monopole resonates at a frequency of 3.5 GHz as shown in Figure 1(b). To make antenna resonate for dual frequencies, extra resonant modes has to be added. So splitting rectangular monopole in Ant 2 creates an additional current path of $\lambda_g/4$ leading to dual-band response [16]. These variable length rectangular strips resonate at two different frequencies. However, the desired dual frequency bands are not achieved. In Ant C, two arms are added to ANT B giving rise to an F-shaped monopole antenna. The lower arm and upper arm combine to produce resonance at 3.5 GHz frequency band whereas upper arm of the F-shape antenna produces resonance at around 5.9 GHz frequency band. To improve the overall impedance matching of the antenna, a rectangular slot is etched at the upper edges of the ground plane below the feed line. The resonating frequency of the proposed antenna is controlled by the dimension of upper and lower arms. The evolution of dual-band F-shaped monopole antenna and its corresponding simulated S-parameter is shown in Figure 1.

The step by step evolution of the proposed dual-band MIMO antenna is shown in Figure 2. Initially the F-shaped dual-band monopole is designed. To accommodate the second element, the dimension of the ground plane is increased, and the second element is placed at 180° with respect to the first element. Thus, Ant 1 consists of two counter-facing F shape monopole antennas with edge to edge separation of $0.1167\lambda_0$ at 3.5 GHz. The radiating element and ground plane both affect the impedance matching of the monopole antenna. So ground plane dimensions are also optimized to achieve the desired dual bands. Thus, $S_{11} < -10\,\text{dB}$ is obtained over 3.2–3.8 GHz and 5.7–6.2 GHz, but mutual coupling is very high over these operating dual bands.

In Ant 2, an elliptical slot is introduced in the middle of ground plane for lowering the mutual coupling at lower operating band. This slot works as a band-stop filter at 3.5 GHz frequency by suppressing the surface wave and improves the isolation over 3.2–3.8 GHz with no improvement in mutual coupling over 5.7–6.2 GHz as shown in Figure 3. In Ant 3, rectangular parasitic strips are added besides the F-shape antenna element. These parasitic strips help to direct the beam in one particular direction and thus reduce the mutual coupling by suppressing the surface and space waves. As a result, $S_{12} < -20\,\text{dB}$ is achieved over the upper band, i.e., 5.7–6.2 GHz. Thus, both elliptical slot and rectangular parasitic strips contribute to high isolation over the operating dual bands. The simulated

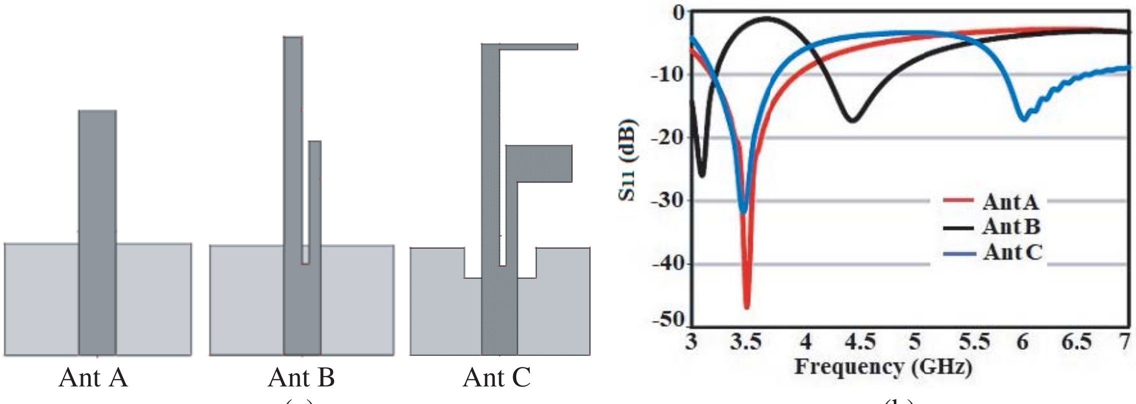

(a) (b)

Figure 1. (a) Evolution of dual band F-shaped monopole antenna and (b) simulated S-parameter.

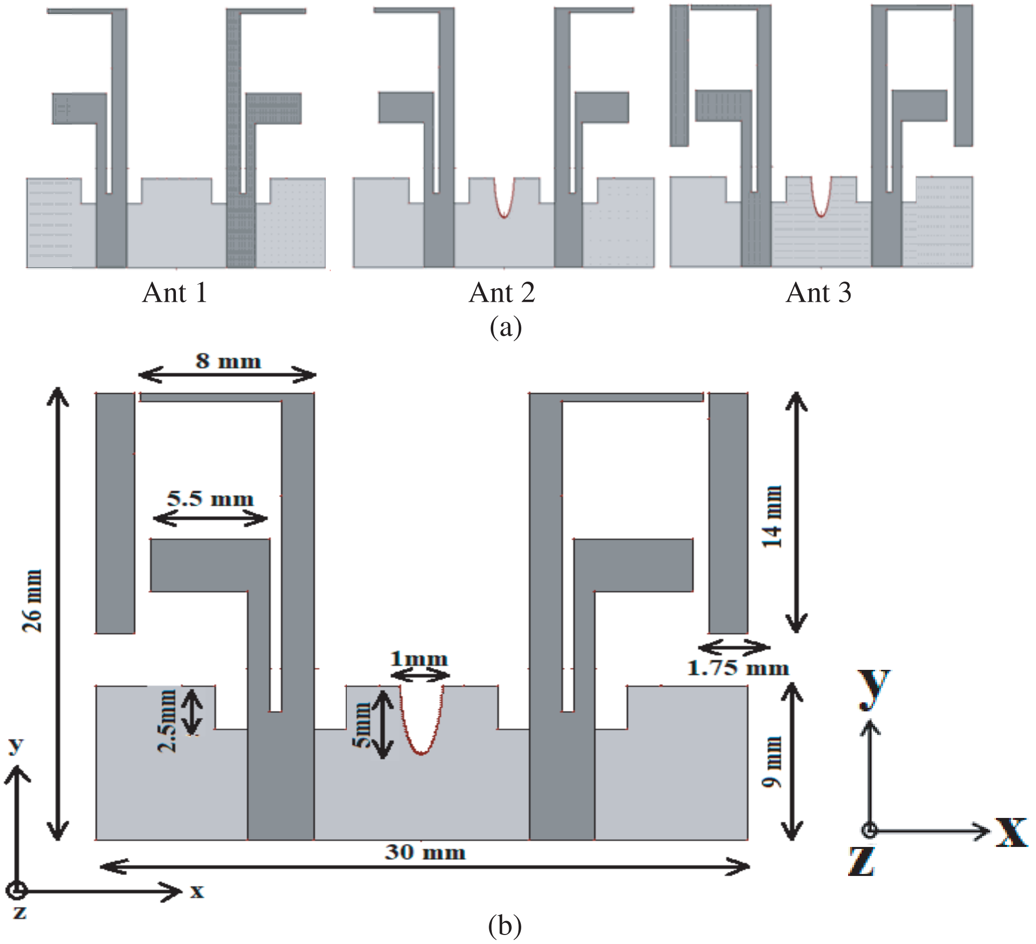

(a)

(b)

Figure 2. (a) Step by step evolution of proposed MIMO antenna and (b) proposed MIMO structure.

S-parameters (S_{11} and S_{12}) of each stage of the proposed MIMO antenna are shown in Figure 3. All the antenna structures are simulated using IE3D software [17] and designed on a 1.6 mm thick FR-4 substrate. The surface current distributions of Ant 1 and Ant 3 at frequency 3.5 GHz and 5.8 GHz are shown in Figure 4. For examining this, port 1 is excited, and port 2 is terminated with match load of

50 Ω. Less amount of current is coupled from port 1 to port 2 in Ant 3 than Ant 1. The current is more intense around the elliptical slot in lower band whereas for upper band, more surface current is induced in rectangular parasitic strips. Thus, both elliptical slot and rectangular parasitic strips help to achieve high isolation over the operating dual bands of the proposed MIMO antenna.

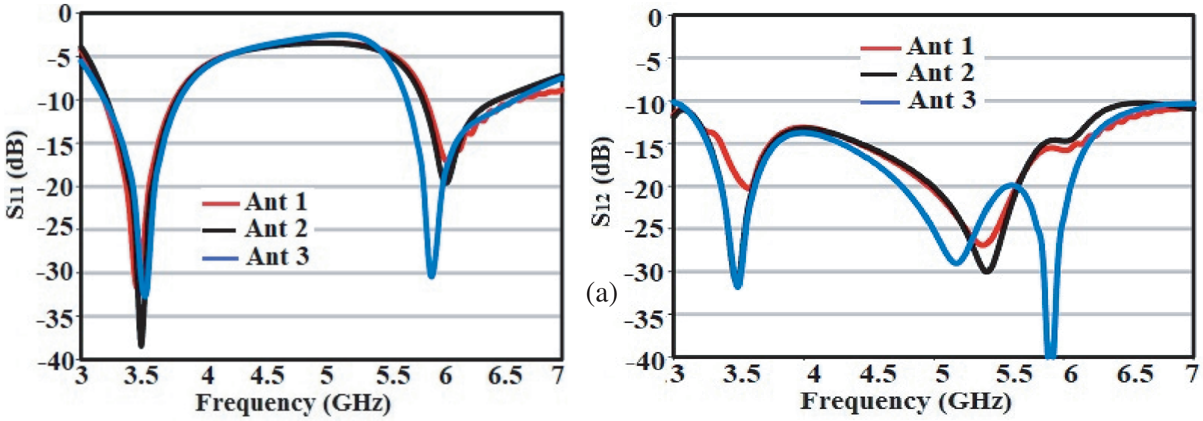

(a) (b)

Figure 3. Simulated (a) S_{11} and (b) S_{12} of all structures.

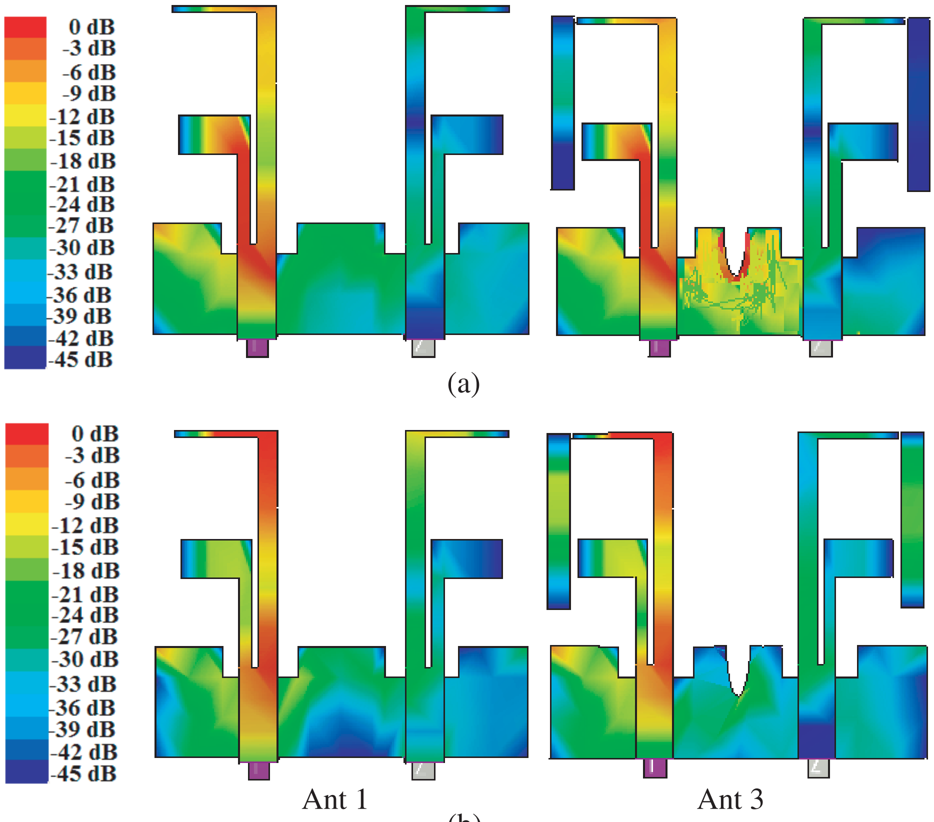

(a)

(b)

Figure 4. Surface current distribution at (a) 3.5 GHz and (b) 5.8 GHz.

2.1. Fabricated Antenna and Measured Results

The proposed MIMO antenna is fabricated on an FR-4 substrate of thickness 1.6 mm as shown in Figure 5. The overall dimensions of the proposed MIMO antenna are 30 mm × 26 mm × 1.6 mm. The fabricated antenna is tested using Agilent 9916 A network analyzer, and the measured results are compared with the simulated ones as shown in Figure 6. There is a slight difference between measured and simulated results due to copper loss, connector loss and errors in fabrication. Impedance bandwidth less than −10 dB and mutual coupling less than −20 dB are obtained over 3.2–3.8 GHz and 5.7–6.2 GHz.

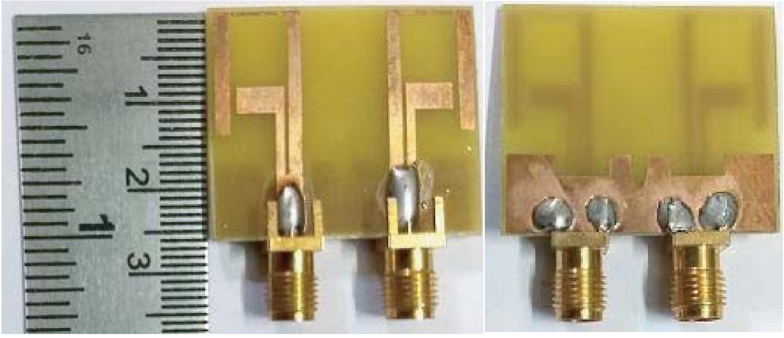

(a) (b)

Figure 5. (a) Top and (b) bottom view of the proposed fabricated MIMO antenna.

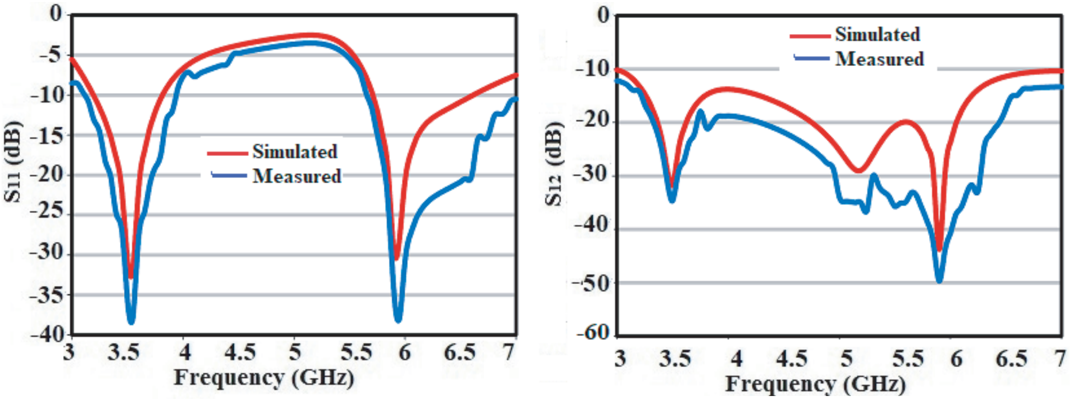

(a) (b)

Figure 6. Measured and simulated S-parameters.

The radiation patterns in XZ plane and YZ plane at 3.5 GHz and 5.8 GHz are shown in Figure 7. For measurements, port 1 is excited while port 2 is terminated with 50 Ω load. The radiation patterns are relatively stable over the impedance bandwidth. The maximum gains of antenna at resonating frequencies 3.5 GHz and 5.8 GHz are 1.5 dBi and 2.8 dBi, respectively as shown in Figure 8(a). The antenna has less gain variation over the operating bands.

The correlation coefficient is a significant parameter in investigating the diversity performance of MIMO antennas. The correlation coefficient can be evaluated from: 1) far-field radiation pattern of antenna and 2) scattering parameter. The correlation coefficient calculated from the antenna field radiation pattern for uniform multipath indoor environment is given by following formula [18]:

$$\rho \frac{\left|\iint_{4\pi}^{0}\left[\vec{F}1\left(\theta,\Phi\right)\cdot\vec{F}2\left(\theta,\Phi\right)d\Omega\right]\right|^{2}}{\left|\iint_{4\pi}^{0}\left[\vec{F}1\left(\theta,\Phi\right)d\Omega\right]\right|^{2}\left|\iint_{4\pi}^{0}\left[\vec{F}2\left(\theta,\Phi\right)d\Omega\right]\right|^{2}} \tag{2}$$

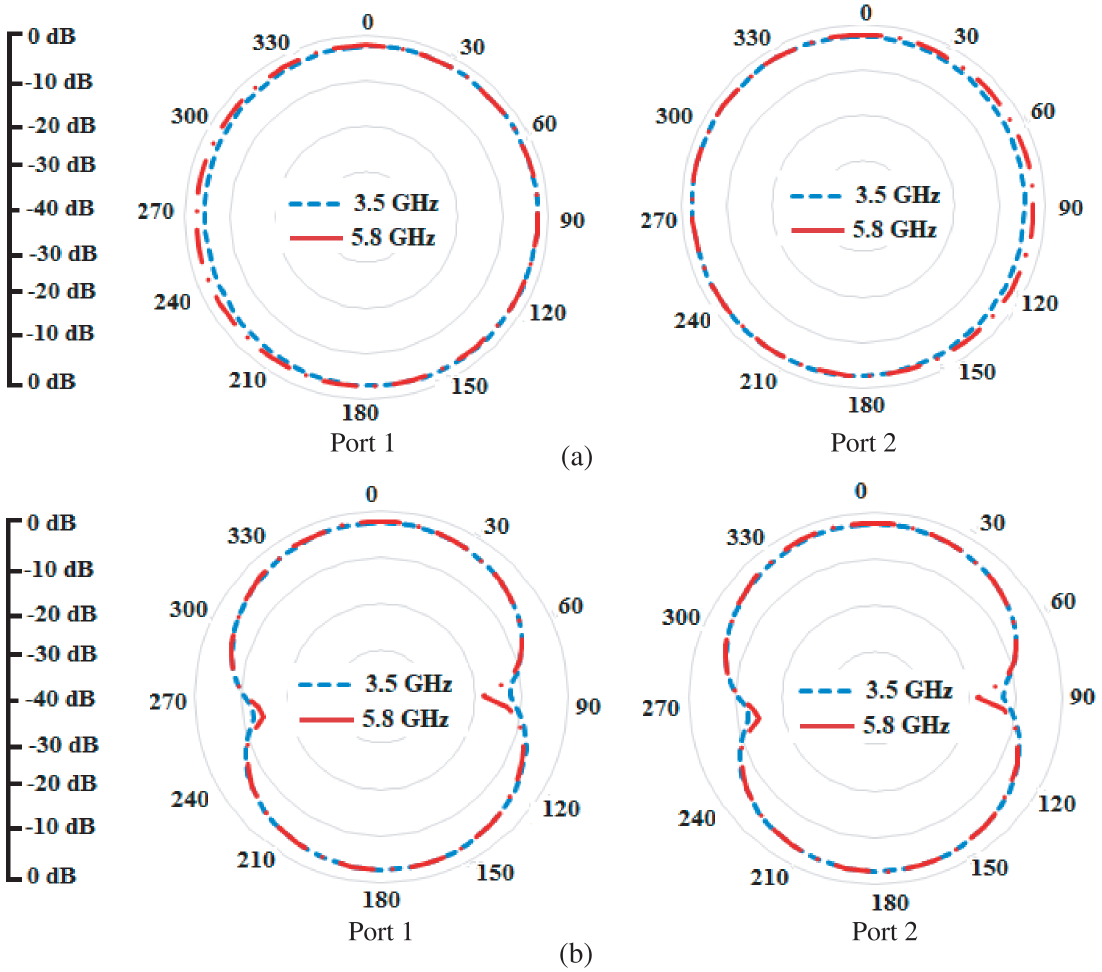

(a)

(b)

Figure 7. Radiation pattern in (a) *X-Z* plane and (b) *Y-Z* plane.

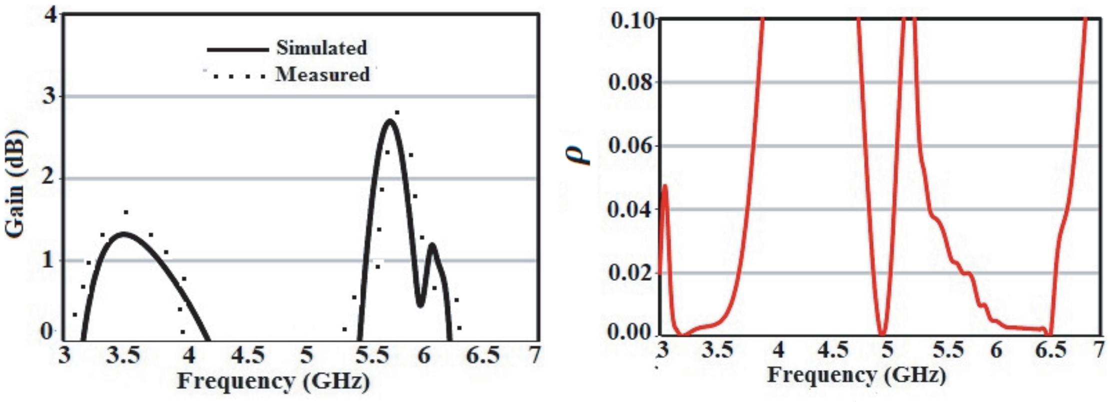

(a) (b)

Figure 8. (a) Gain and (b) correlation coefficient of the proposed structure.

where the symbol (·) represents the Hermitian product; Ω denotes the solid angle; F( ) denotes the antennas field radiation pattern obtained by exciting one port while the other port is terminated by load of 50 ohms. The method of calculating the correlation coefficient from the radiation pattern of antenna is a very tedious process, and it is difficult to analyze as it deals with complex calculation and numerical integration. The second way of evaluating correlation coefficient is by using its equivalent S-parameter based on the assumption that the antennas are lossless. It is calculated using the following formula [18]:

$$\rho = \frac{\left|S_{11}^{*}S_{12} + S_{21}^{*}S_{22}\right|^2}{\left(1 - \left(\left|S_{11}\right|^2 + \left|S_{21}\right|^2\right)\right)\left(1 - \left|S_{22}\right|^2 + \left|S_{12}\right|^2\right)\right)} \tag{3}$$

Equation (3) is the simplest form of Equation (2). This method of calculating correlation coefficient is very simple and gives more accurate result in multipath indoor propagation environment. The correlation coefficient should be less than 0.5 to achieve significant diversity among MIMO antenna elements [19]. The correlation coefficient of proposed antenna is less than 0.03 for both operating bands

Table 1. Comparison of proposed antenna with reference antennas.

Ref.	**Frequency Band (GHz)**	**Isolation (dB)**	**Technique Used**	**Max. Gain (dB)**	**Size (mm^2)**
5	2.4–2.6 5.2–6	17 20	Neutralization line	4	40 × 80
6	2.34–2.55 5.13–5.85	20 20	T shaped junction and slots	NR	38 × 43
7	2.1–2.7 5.1–6.1	15 20	Slots and Trident Structure	4.4	40 × 90
8	2.2–2.7 4.6–5.9	20 15	Modified T-shape Resonator	4.5	40 × 40
9	2.38–2.52 3.19–6.44	15 15	Orthogonal placement of antenna	2.9	42 × 62
10	2.4–2.5 5.725–5.875	20 20	Stub and Strip	4.86	50 × 65
11	2.4–2.5 5–5.5	20 30	CSRR	4	70 × 90
12	2.26–2.5 5.41–5.79	20 20	Slots and Transmission lines	4.34	30 × 65
13	2.3–2.5 5.725–5.875	20 20	Decoupling Structure	NR	70 × 40
14	3.32–3.74 5.45–6.05	20 20	T shaped Structure and slots	2.8	30 × 30
Proposed	3.2–3.8 5.7–6.2	20 20	Elliptical slot and rectangular parasitic strip	2.8	30 × 26

as shown in Figure 8(b). The diversity gain is calculated using correlation coefficient as follows [20]:

$$G_{app} = 10 \times \sqrt{1 - |\rho|} \tag{4}$$

The diversity gain for both bands is greater than 9.8 dB as shown in Figure 9.

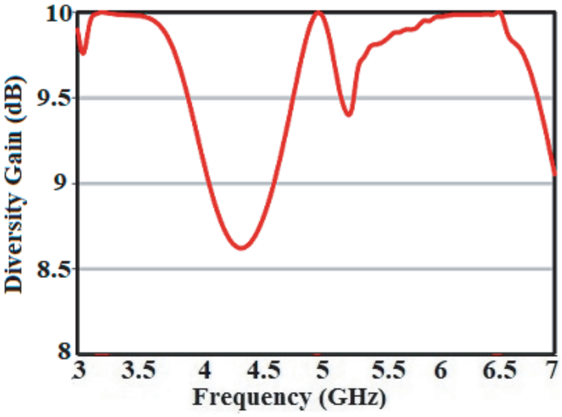

Figure 9. Diversity gain of the proposed structure.

The proposed antenna is compared with the antennas reported in the literature in Table 1. It indicates that the proposed dual-band antenna has smaller size than that of other reported antennas. The antenna has mutual coupling $< -20\,\text{dB}$, ECC < 0.03 with stable radiation pattern over the operating dual bands. The proposed antenna is easy to design and has used simple isolation techniques. Therefore, the proposed dual band antenna is suitable for MIMO applications.

3. CONCLUSION

A dual-band MIMO antenna with improved isolation is proposed in this paper. Mutual coupling is reduced using an elliptical slot and a rectangular parasitic strip. $S_{11} < -10\,\text{dB}$ is obtained over 3.2–3.8 GHz and 5.7–6.2 GHz with $S_{12} < -20\,\text{dB}$. The proposed dual-band MIMO antenna is simple to design. The dimension of the proposed dual-band MIMO antenna is $30 \times 26\,\text{mm}^2$. The antenna has ECC < 0.03, diversity gain $> 9.8\,\text{dB}$ and stable radiation patterns over the operating bands. Thus, the proposed dual-band MIMO antenna is an appropriate candidate for WI-MAX and WLAN applications.

REFERENCES

1. Jensen, M. A. and J. W. Wallace, "A review of antennas and propagation for MIMO wireless communications," *IEEE Transactions on Antennas and Propagation*, Vol. 52, No. 11, 2810–2824, Nov. 2004.
2. Ozdemir, M. and E. Arvas, "Dynamics of spatial correlation and implications on MIMO systems," *IEEE Commun. Mag.*, Vol. 42, No. 6, S14–S19, Jun. 2004.
3. Palandoken, M., "Artificial materials based microstrip antenna design," *Microstrip Antennas*, InTech, 2011.
4. Palandoken, M., "Dual broadband antenna with compact double ring radiators for IEEE 802.11ac/b/g/n WLAN communication applications," *Turkish Journal of Electrical Engineering and Computer Sciences*, 10.3906/elk-1507-121, 2017.
5. Huang, J. H., W. J. Chang, and C. F. Jou, "Dual-band MIMO antenna with high isolation application by using neutralizing line," *Progress In Electromagnetics Research Letters*, Vol. 48, 15–19, 2014.
6. Qin, H. and Y. Liu, "Compact dual-band MIMO antenna with high port isolation for WLAN applications," *Progress In Electromagnetics Research C*, Vol. 49, 97–104, 2014.

7. Roshan, R. and R. K. Singh, "Dual ISM band MIMO antenna for WiFi and WiMax application," *International Conference on Signal Propagation and Computer Technology (ICSPCT)*, 209–213, 2014.
8. Liu, Y., L. Yang, Y. Liu, J. Ren, J. Wang, and X. Li, "Dual-band planar MIMO antenna for WLAN application," *Microwave Opt. Technol. Lett.*, Vol. 57, No. 10, 2257–2262, Oct. 2015.
9. Desde, I., G. Bozdag, and A. Kustepeli, "Multi-band CPW-fed MIMO antenna for bluetooth WLAN and WiMAX applications," *Microw Opt. Tech. Lett.*, Vol. 58, No. 9, 2182–2186, 2016.
10. Ding, Y., Z. Du, K. Gong, and Z. Feng, "A novel dual-band printed diversity antenna for mobile terminals," *IEEE Transactions on Antennas and Propagation*, Vol. 55, No. 7, 2088–2096, 2007.
11. Yang, D. G., D. O. Kim, and C.-Y. Kim, "Design of dual-band MIMO monopole antenna with high isolation using slotted CSSRR for WLAN," *Microw. Opt. Technol. Lett.*, Vol. 56, 2252–2257, 2014.
12. Cui, S., Y. Liu, W. Jiang, and S. X. Gong, "Compact dual-band monopole antennas with high port isolation," *Electron. Lett.*, Vol. 47, No. 10, 579–580, May 12, 2011.
13. Jiang, W., L. Yang, B. Wang, and S. Gong, "A high isolation dual-band MIMO antenna for WLAN application," *2017 International Symposium on Antennas and Propagation (ISAP)*, Oct. 30–Nov. 2, 2017.
14. Zhao, N. and W.-P. Tian, "CPW-fed dual-band MIMO antenna with common radiating element," *Progress In Electromagnetics Research Letters*, Vol. 62, 71–75, 2016.
15. Ray, K. P., "Design aspects of printed monopole antennas for ultra-wide band applications," *International Journal of Antennas and Propagation*, Vol. 2008, 1–8, Mar. 2008.
16. Ali Nezhad, S. M. and H. R. Hassani, "A novel triband E-shaped printed monopole antenna for MIMO application," *IEEE Antennas and Wireless Propagation Letters*, Vol. 9, 576–579, 2010.
17. IE3D Release 14, Zeland Software Inc., Fremont, CA, USA, 2008.
18. Blanch, S., J. Romeu, and I. Corbella, "Exact representation of antenna system diversity performance from input parameter description," *Electron. Lett.*, Vol. 39, No. 9, 705–707, May 2003.
19. Ko, S. C. K. and R. D. Murch, "Compact integrated diversity antenna for wireless communications," *IEEE Trans. Antennas Propagation*, Vol. 49, No. 6, 954–960, 2001.
20. Rosengren, K. and P. Kildal, "Radiation efficiency, correlation, diversity gain and capacity of a six-monopole antenna array for a MIMO system: Theory, simulation and measurement in reverberation chamber," *IEE Proc., Microw. Antennas Propag.*, Vol. 152, No. 1, 7–16, 2005.